

EXPERIMENTAL STUDY OF LOSSES IN DOUBLY-FED INDUCTION GENERATOR

Vladimir Lazarov, Zahari Zarkov and Ludmil Stoyanov

ЕКСПЕРИМЕНТАЛНО ИЗСЛЕДВАНЕ НА ЗАГУБИТЕ В ДВОЙНО ЗАХРАНВАН АСИНХРОНЕН ГЕНЕРАТОР

Владимир Лазаров, Захари Зарков, Людмил Стоянов

Abstract: This paper presents an experimental study of the losses doubly-fed induction generator (DFIG) for wind energy conversion system. The experiments were performed on a laboratory test bench. The losses in the components of the system - electronic converters, transformer and induction machine - are determined by measuring the power in different system points and by making the appropriate calculations. Quantitative assessment of the distribution of losses and of the overall system efficiency is also carried out. The results can serve to validate the theoretical models and assumptions. Although the study is designed for a small power machine, it makes it possible to outline certain trends and connections between the losses and the energy flows in systems with DFIG.

Keywords: DFIG, losses, wind generator

INTRODUCTION

Over the past 10 years, wind generators (WG) and farms have become a serious alternative to conventional power plants. The development of more powerful machines and continuous installation of new capacities give reason to believe that development in this area will continue at similar rates [1]. Currently, one of the most popular machines used in wind farms are wound rotor induction generators (IG) with rotor side control, also known as doubly-fed IG (DFIG) [2]. DFIGs are manufactured with powers exceeding 3MW and have performed well in practice. Many wind generators of this type have been installed in Bulgaria. There are 20 units of DFIG with 2,5MW capacity each installed on the ridge of the Balkan Mountains.

Much of the academic research in DFIG, has focussed on modelling systems with DFIG, but usually without taking into accounts all peculiarities of the machines. Mechanical losses and iron losses are usually ignored because this leads to very complicated models. The models typically take into account only losses in the active resistance of the windings [3], [4]. The situation is similar with the other elements of the systems - electronic converters, filters and transformers [5]. Again, the analytical determination of losses is difficult. It is not possible to ignore these losses in practice and therefore, a detailed understanding of these losses is necessary.

Although the power converted in the rotor circuit is up to 30% of the stator power [6], the losses in converters, filters and in the transformer cannot be

ignored and require more detailed investigation. This is also necessary for the design of the machinery and electronic converters cooling systems.

The goal of this paper is to study experimentally and to quantify the losses in the components of a system for generating electricity using a low power DFIG. For this purpose, measurements were made of powers in different system points under different operating modes and the appropriate calculations were performed to determine the losses. This allows for estimation of the error that is made when ignoring the losses in the simulation models.

BASICS

The structure of the studied system with DFIG is shown in Fig.1. The system is a laboratory test bench. The power from the rotor circuit is exchanged with the grid through reversible power electronic converter, consisting of two voltage source converters (VSC) controlled by pulse-width modulation (PWM) - structure "back-to-back".

The authors' goal is to measure and calculate the powers in this system at all key points - before and after each power converter - and then to directly calculate the losses in the respective converter.

To this end and wherever possible, the authors have made separate studies of the losses in the device and found the relevant dependencies.

The test system with DFIG consists of the following elements:

- Wound rotor induction generator (WRIG);
- Variable-speed DC motor with known characteristics, replacing the real wind turbine;

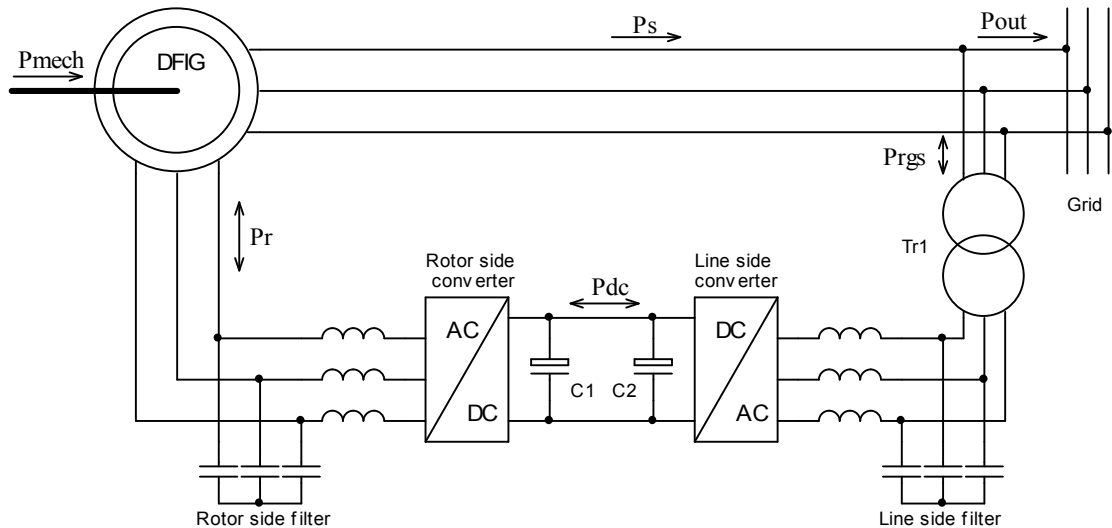


Fig. 1. Circuit of the test bench.

- Electronic converter at the rotor side, which consists of three-phase voltage-source controller (VSC) with MOSFETs and LC filter;
- Electronic converter at the line side – also three-phase VSC with MOSFETs and LC filter;
- Three-phase transformer as a link between the line side VSC and the grid;
- Current and voltage sensors at appropriate places in the system.

A general view of the test bench is shown in Fig. 2.

The control of the power converters is performed by a dSPACE 1103 microprocessor system. The measurements of powers in different system points were made for various operation modes – subsynchronous and super synchronous generator rotation speed. The waveforms of currents and

voltages at the rotor side were recorded using a digital oscilloscope and then the average power was calculated. For the points where voltage and current sensors exist simultaneously (on the grid side and at DC link), measurements were performed in real time using dSPACE control system.

POWER LOSSES IN SYSTEM ELEMENTS

In order to maximise the precision of results, the elements of the system were tested individually. The first device is **the transformer**. Its rated power is 600VA and rated secondary phase voltage is 14.4V. The losses in the transformer consist of two parts – iron losses and copper losses. The first are invariant at constant supply voltage and the second depend on the windings' current and transferred power

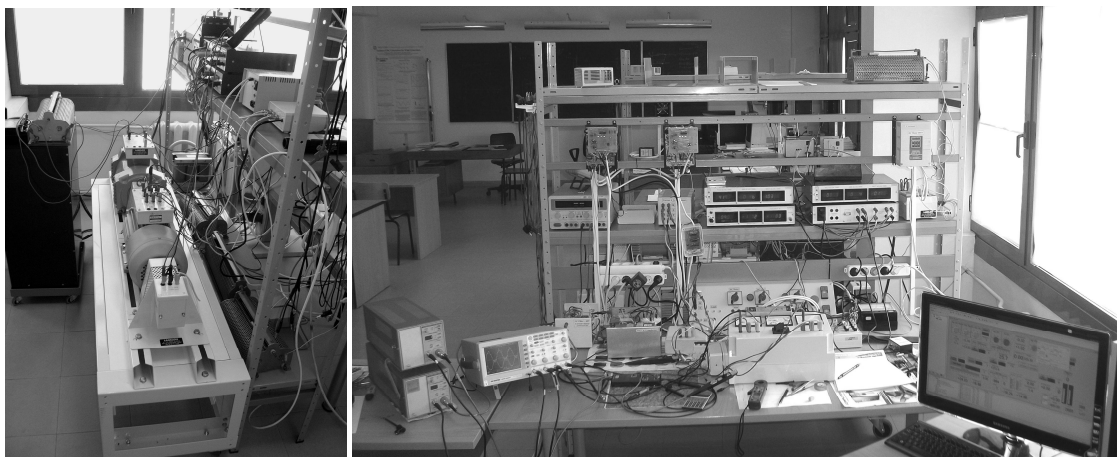


Fig. 2. General view of the test bench with the control system.

respectively. The following numbers are obtained as a result of the measurements.

Iron losses at phase voltage $V_g=235V$ are $P_{itr}=13.2W$.

Transformer copper losses P_{tr_cop} in function of the transferred power (of the grid side) are shown in Fig. 3.

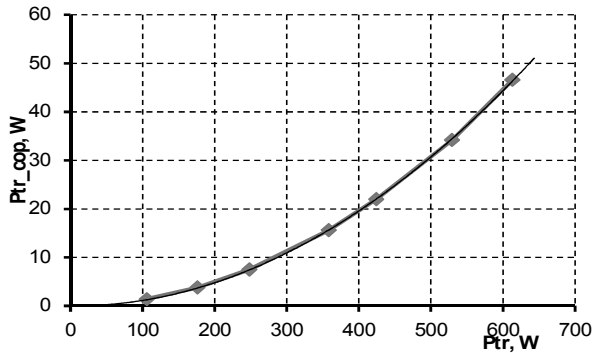


Fig. 3. Copper losses in the transformer.

Machine losses

The generator has been tested and different types of losses are measured and calculated. It is done by well-known procedure for losses determination in an electrical machine [7]. The primary mover is a DC motor with known characteristics.

The data of the induction machine (IM) are the following:

- Rated power $P=1500W$;
- Rated speed 1500rpm; pole number – 4;
- Rated voltage 400V, star connection;
- Rated current (as a motor) 3.6A;
- Stator winding resistance 3.1Ω at $20^\circ C$;
- Rotor winding resistance including the slip ring contact 0.164Ω at $20^\circ C$.

Hereinafter the results from the measurements and losses calculations are presented.

Induction machine mechanical losses P_{mg} are derived when the external motor rotates the IM and the mechanical power P_{mech} at the shaft is measured. The IM is not excited, i.e. no currents flow through the windings – all windings are open. We can consider that

$$(1) \quad P_{mg} = P_{mech}$$

where P_{mg} are the mechanical losses in the IM. These losses as a function of the speed of rotation are shown in Fig. 4.

Iron losses in the IM P_{iron} are determined as follows. The machine is rotated by the external motor, the stator winding is connected to the three-phase grid with phase voltage $V_g=235V$ and the rotor winding is open. The measurements are done

for the electrical power consumed from the grid P_{el} and for the mechanical power on the shaft of the IM P_{mech} . All input power is spent for covering the mechanical losses P_{mg} , the iron losses in the IM and stator copper losses P_{els} . Therefore, we have

$$(2) \quad P_{mech} + P_{el} = P_{mg} + P_{iron} + 3.R_s.I_s^2 \quad \text{and}$$

$$P_{iron} = P_{mech} + P_{el} - P_{mg} - 3.R_s.I_s^2$$

where I_s is the stator current and R_s is the stator winding resistance.

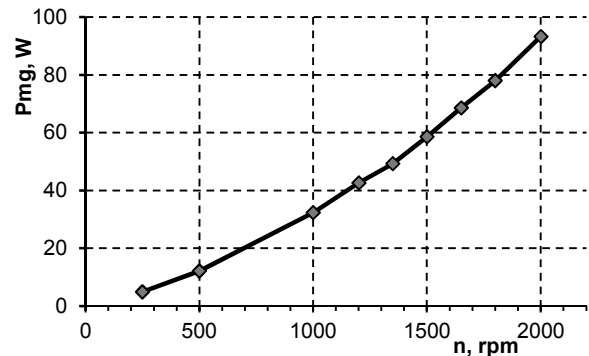


Fig. 4. Mechanical losses of the induction machine vs. speed.

P_{mg} being already known we can calculate P_{iron} . Iron losses in the IM at different rotation speeds are shown in Fig. 5. The constant stator voltage leads to constant stator current. This current is magnetizing for the machine and can be considered constant. The figure shows that the losses increase with the rotation speed above the synchronous velocity.

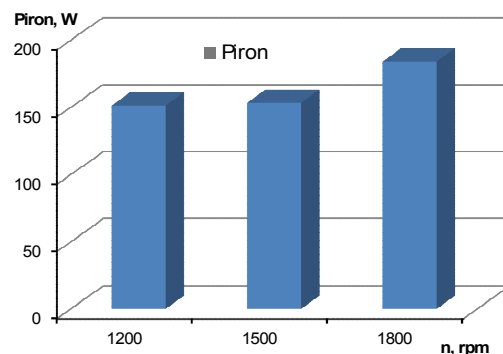


Fig. 5. Iron losses in the IM excited by the stator current vs. speed.

Another experiment for determination of the iron losses has also been done. The stator of the IM was connected to the grid but with short-circuited rotor. Then the machine was rotated by the DC motor so as the electrical power consumed from the grid was zero. The rotation speed was slightly higher than synchronous

1507 rpm – necessary to put the machine in generator mode. In this case, all losses in the IM are covered by the mechanical power coming from the shaft

$$(3) \quad P_{iron} = P_{mech} - P_{mg}$$

The result is 157.4W compared to 153.5W with open rotor circuit. The difference is only 2.5%.

Other experiments were carried out but with excitation of the IM from the rotor side, that is the real case in using DFIG. The IM was rotated by the external motor with open stator winding and supplied rotor winding. The rotor currents were synchronised with the slip frequency so that the resulting magnetic flux rotates with synchronous speed [8]. This is possible using the rotor side electronic converters with current control, which adjusts the rotor current magnitude and frequency.

The electrical power consumed by the rotor P_r and the mechanical power from the motor P_{mech} were measured. These powers cover the mechanical losses, the copper losses in the rotor and the iron losses in the machine

$$(4) \quad P_{mech} + P_r = P_{mg} + 3R_r I_r^2 + P_{iron} \Rightarrow \\ \Rightarrow P_{iron} = P_{mech} + P_r - P_{mg} - R_r I_r^2$$

where I_r is the rotor current RMS value and R_r is the rotor winding resistance.

Thus, the iron losses were determined as a function of the speed and rotor current. The results are shown in Fig. 6 where I_{rm} is the magnitude of rotor current.

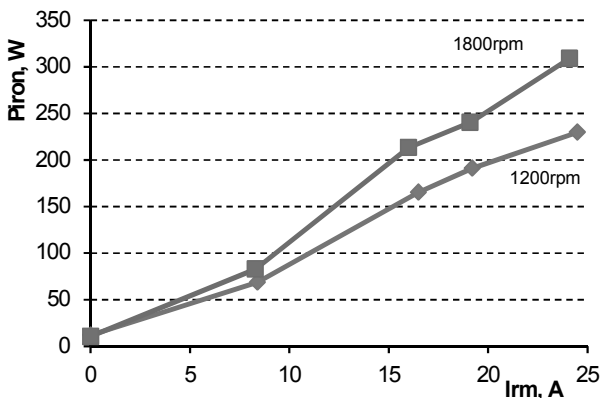


Fig. 6. Iron losses in the IM vs. rotor current at 1200 and 1800rpm.

In Fig. 7 are shown the IM iron losses as a function of the speed at constant rotor current $I_{rm} = 19.2A$. This value of the current is chosen because it produces 235V stator voltage that can be considered as nominal for all experiments in this study. Consequently, the machine flux and corresponding rotor current also have nominal values.

The curve in Fig. 7 has a visible minimum at the synchronous speed (1500 rpm). The possible reason is the absence of iron losses in the rotor when the slip is zero [9].

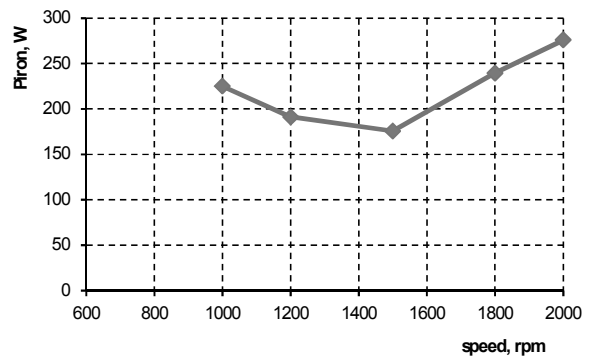


Fig. 7. Iron losses in the IM vs. speed at constant rotor current.

Electronic converter losses

The losses in both electronic converters are calculated as a difference between measured powers in the rotor-side chain: grid – transformer – grid-side VSC – rotor-side VSC – rotor. The powers were measured at three points – at the grid side P_{rgs} , at the DC link P_{DC} and at the output of the rotor VSC P_r (see Fig.1). Consequently, we have

$$(5) \quad P_{tr} + P_{VSCg} = P_{rgs} - P_{DC}$$

$$(6) \quad P_{VSCr} = P_{DC} - P_r$$

where the transformer losses are denoted by P_{tr} , the grid-side VSC losses are denoted by P_{VSCg} and losses in the rotor-side VSC – by P_{VSCr} .

Fig. 8 shows the losses in the rotor side VSC including the filter. The values are relatively small because of the very low on-resistance of the MOSFET transistors used in the rotor side VSC – about 5mΩ. Therefore, a big portion of this loss occurs in the choke of the filter.

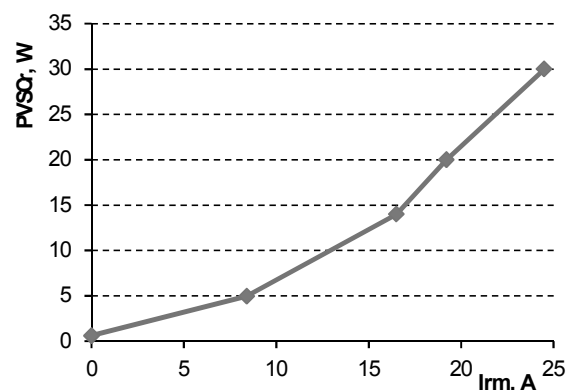


Fig. 8. Power loss in rotor side VSC vs. magnitude of the rotor current.

Fig. 9 shows the sum of the losses in the transformer and in the grid side VSC including the filter. The values are presented as a function of the grid-side power of the transformer P_{rgs} . That way the results are more easily usable in future studies because the power on the grid-side of the rotor converters is always measured. The curve in Fig. 9 does not tend to zero because of transformer core losses that remain constant even at zero power.

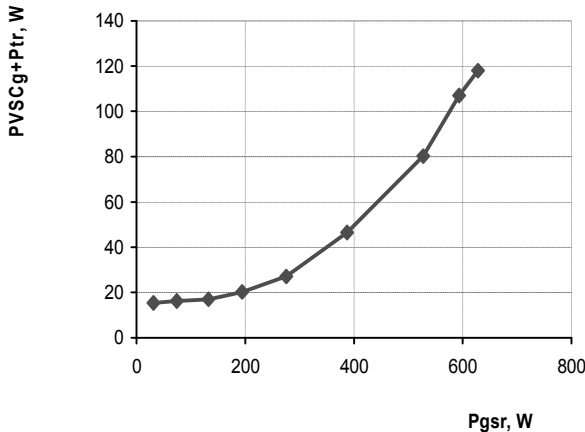


Fig. 9. Total losses in the grid side VSC and in transformer vs. the grid-side transformer power.

DISTRIBUTION OF POWER LOSSES IN THE SYSTEM

A set of experiments was done to identify the distribution and variation of losses in the whole DFIG system with the change of speed and stator power of the generator. The control system allows the independent control of active and reactive stator power of the machine. During the experiments, the stator reactive power was set to zero and active power was changed. Characteristics for different speeds and powers were obtained this way.

The results of the experiments are presented below. The losses in the system at sub-synchronous speed and a given stator power are shown in Table 1 as numbers and as percentage of total losses sum. The same results are also presented in Fig. 10.

Table 1. Losses distribution at 1200 rpm and stator power 1065W

	P_{mg}	P_{elr}	P_{VSCr}	P_{VSCg}	P_{iron}	P_{els}
Watt	42.6	147.1	64.6	107.0	244.1	22.3
%	6.8	23.4	17.0	10.3	38.9	3.6

Fig. 11 shows the losses variation in function of the stator power P_s at constant speed 1200 rpm. Fig. 12 shows the change of input mechanical power

P_{mech} , electrical power of the rotor side P_{rgs} and total output power of the DFIG P_{out} . The same experiment was also done for supersynchronous speed 1800 rpm.

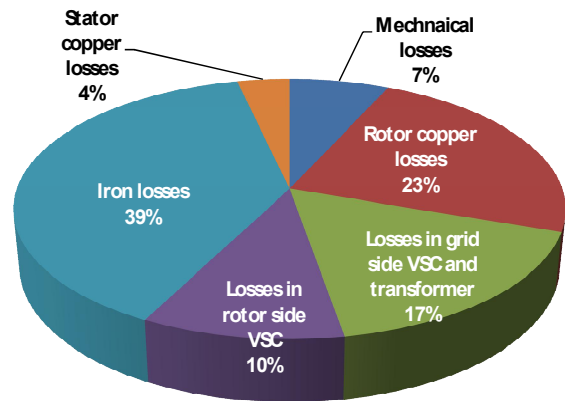


Fig. 10. Loss distribution at n=1200 rpm, Ps=1065W.

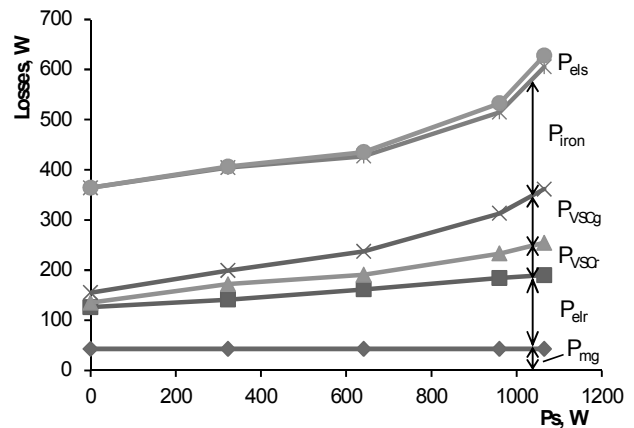


Fig. 11. Losses variation vs. stator power at speed 1200 rpm.

From these results, it can be concluded that the main losses occur in the machine core (iron losses). Moreover, they increase because of higher current harmonics due (mainly) to the electronic converter connected to the rotor. In this particular machine, the rotor copper losses are relatively big and this is because the machine is designed for a motor. The rotor coil is not intended to carry the magnetizing current component and has greater resistance. This leads to increased copper losses in the rotor during the operation of the machine in DFIG configuration. On the other hand, the copper losses in the stator are almost negligible. The losses in the grid-side VSC and transformer are also considerable and increase with the square of the rotor power.

In Fig. 12, it can be seen how the rotor power increases with the rise of the stator power.

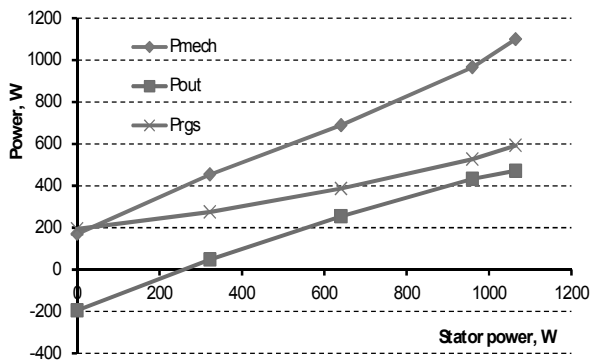


Fig. 12. Power variation vs. stator power at speed 1200 rpm.

Another experiment was done to reveal the dependence of losses on the speed of rotation. During the measurements, the stator power was constant. The rotor power, output power and input mechanical power vary as shown in Fig. 13.

In Fig. 14 the authors summarize the power losses at different speeds of rotation. It is clearly visible that the losses are minimal around the synchronous speed (1500 rpm) and near above it.

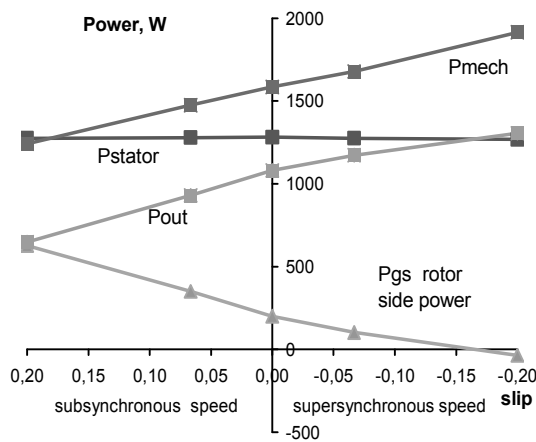


Fig. 13. Power variation and overall efficiency vs. the slip at constant stator power.

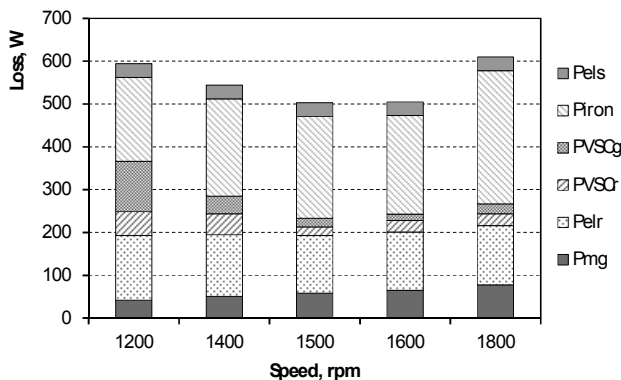


Fig. 14. Loss distribution vs. speed at stator power 1275 W.

Additionally, calculations are made for the efficiency of the whole system under different operating conditions. The results for constant speeds and variable stator power are shown in Fig. 15.

The curves have the usual form. Efficiency levels at a higher speed are much bigger that at a subsynchronous speed. It is normal because of lower power exchanged via the rotor circuit and lower losses in the electronic converters, transformer and in the rotor windings.

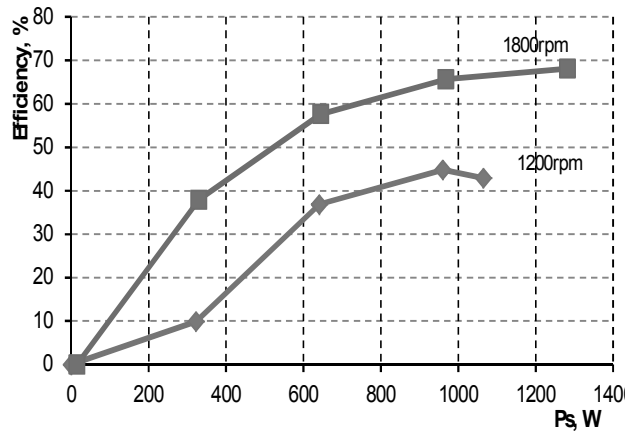


Fig. 15. Overall efficiency of the system at constant speed.

A comparison of the efficiency at different speeds (slips) is depicted in Fig. 16. The efficiency is obtained with constant stator power while the total power P_{out} varies with the slip (Fig. 13).

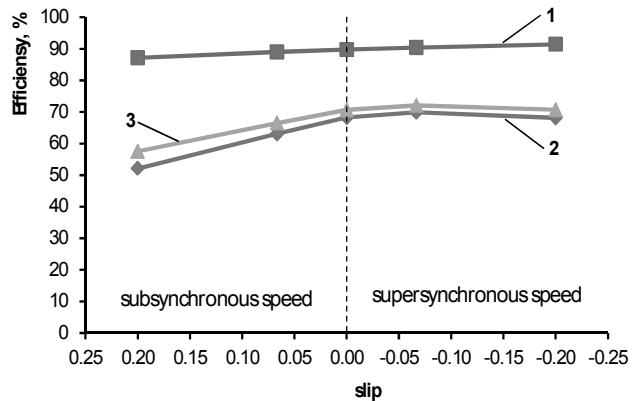


Fig. 16. Comparison of the overall efficiency of the system at different speeds: 1 – simulated result; 2 – experimental result; 3 – predicted result, taking into account the mechanical, iron and converter losses.

Fig. 16 also shows a simulated curve of the efficiency. The simulations were made with a model of a whole DFIG system [4] under the same conditions used for the experiments. The calculated efficiency by the model is higher than that observed

experimentally. Curve 3 in Fig. 16 shows the predicted efficiency calculated by the simulated results by adding the mechanical, iron and converter losses. It has a quite good agreement with the experimental results.

These results indicate that the simulation model can be successfully updated taking into account the neglected losses in the DGIF system.

CONCLUSION

The purpose of the paper was to study experimentally and to quantify the losses in the components of a system for generating electricity using low power DFIG. By measuring the powers at different system points under different operating modes and the appropriate calculations, the losses in each component of the system - electronic converters, transformer and induction machine - were determined.

Quantitative assessment of the losses distribution and of the overall system efficiency was carried out.

The results can serve to validate theoretical models and assumptions made in them. This allows for estimation of the error that is made in simulations when ignoring the losses in the some system components.

Taking into account the peculiarities, they may also relate to large machines. Although the studies have been done for a small power machine, they allow for the outline of certain trends and links between the losses and the energy flows in systems with DFIG.

Acknowledgements: The authors wish to thank the National Research Fund for the financial support in

Vladimir Lazarov

Faculty of Electrical Engineering
“Laboratory on Renewable Energy Sources”
Head of the Electrical Machines Department
Technical University – Sofia
8, Kl. Ohridski Blvd.
1000 Sofia, Bulgaria
e-mail: vl_lazarov@tu-sofia.bg

the frame of the programme of the University Research Complex - contract DUNK 03/1.

REFERENCES

- [1] Muyeen, S.M. Wind Energy Conversion Systems. Technology and Trends. Springer-Verlag, 2012.
- [2] Blaabjerg, F., F. Iov, T. Kerekes, R. Teodorescu. Trends in Power Electronics and Control of Renewable Energy Systems. Proc. of Int. Conf. EPE-PEMC 2010, 6-8 September 2010, Ohrid, Macedonia, pp. K1-K19.
- [3] Lazarov, V., L. Stoyanov, K. Bundeveva, Z. Zarkov, D. Spirov. Modelling and simulation of wound rotor induction generator. Proceedings of the Technical University – Sofia, vol. 59, book 2, pp. 94-102, 2009.
- [4] Lazarov, V., G. Notton, L. Stoyanov, Z. Zarkov. Modeling of Doubly Fed Induction Generator with Rotor-side Converter for Wind Energy Conversion Application. Proc. of the Technical University – Sofia, vol. 60, book 1, pp. 289-298, 2010.
- [5] Müller, S., M. Deicke, R.W De Doncker. Doubly fed induction generator systems for wind turbines. IEEE Ind. App. Magazine, May-June 2002, pp.26-33.
- [6] Smith, G.A., K.A. Nigim. Wind-energy recovery by a static Scherbius induction generator. IEE Proc. Vol.128, Pt. C, No. 6, Nov. 1981, pp.317-324.
- [7] Dimitrov, D., et. all. Guide for electrical machines testing. Technica, Sofia, 1991 (in Bulgarian).
- [8] Cuniere, A. Study and control of doubly fed induction machine. Application in wind generators. La Revue 3EI, No. 38, Sept. 2004, pp. 36-44 (in French).
- [9] Boldea, I. Variable Speed Generators. CRC Press, 2005.

Zahari Zarkov

Faculty of Electrical Engineering
Technical University – Sofia
8, Kl. Ohridski Blvd.
1000 Sofia, Bulgaria
e-mail: zzza@tu-sofia.bg

Ludmil Stoyanov

Faculty of Electrical Engineering
Technical University – Sofia
8, Kl. Ohridski Blvd.
1000 Sofia, Bulgaria
e-mail: stoyanov_ludmil@abv.bg